

Onset of the nonlinear dielectric response of glasses in the two-level system model.

J. Le Cochec and F. Ladieu

DSM/DRECAM/LPS, C.E. Saclay, 91191 Gif sur Yvette Cedex, France

(Dated: March 22, 2024)

We have calculated the real part ϵ'' of the nonlinear dielectric susceptibility of amorphous insulators in the kHz range, by using the two-level system model and a nonperturbative numerical quantum approach. At low temperature T , it is first shown that the standard two-level model should lead to a decrease of ϵ'' when the measuring field E is raised, since raising E increases the population of the upper level and induces Rabi oscillations cancelling the ones induced from the ground level. This predicted E -induced decrease of ϵ'' is at odds with experiments. However, a good agreement with low-frequency experimental nonlinear data is achieved if, in our fully quantum simulations, interactions between defects are taken into account by a new relaxation rate whose efficiency increases as E , as was proposed recently by Burin et al. (Phys. Rev. Lett. 86, 5616 (2001)). In this approach, the behavior of ϵ'' at low T is mainly explained by the efficiency of this new relaxation channel. This new relaxation rate could be further tested since it is shown that it should lead: i) to a completely new nonlinear behavior for samples whose thickness is ~ 10 nm; ii) to a decrease of nonequilibrium effects when E is increased.

PACS numbers: 61.43.Fs, 77.22.Ch, 72.20.Ht

Amorphous materials exhibit universal anomalous properties at low temperature. In 1971, Zeller and Pohl [1] discovered below 1 K a quasilinear behavior of the specific heat in a number of glasses contrasting with the Debye law of crystalline materials. Anderson, Halperin, Varma [2] and Phillips [3] proposed an explanation based upon the existence of localized two-level systems (TLS). Their origin may be due to the tunneling of atoms or groups of atoms between two equilibrium positions separated by a narrow energy barrier featuring asymmetric two-well potentials. They are assumed randomly distributed in energy splittings and tunneling barriers as a consequence of the structural disorder of these materials. This model has proven to be successful to understand most salient experimental features.

The standard TLS model assumes defects do not interact with one another. However, defects are strongly coupled to their environment and can emit or absorb phonons. It leads to an indirect interaction between nearest neighbors via the phonon field [4]. Certain recent failures to explain nonequilibrium data (at a few kHz) [5] underscore the likely involvement of these interactions below 100 mK. However, these nonequilibrium effects are small corrections of the kHz stationary response, and, up to recently, examples of stationary susceptibilities strongly affected by interactions were very rare: in the kHz regime, it was argued that the ultra-low- T ($T \sim 1$ mK) plateau of the dielectric constant in the linear regime, strongly different from the expected logarithmic increase, resulted from interactions [6]. Very recently, such a conclusion was drawn from internal friction experiments [7].

In this work, we show that including interactions in the TLS model with a recently proposed mechanism [8] strongly affects the nonlinear stationary dielectric susceptibility ϵ'' of amorphous insulators at a few kHz. A very complete set of such data was published a few years ago by Rogge et al. [9], twenty years after the pioneering work of Frossati et al. [10]. In the linear regime, ϵ'' decreases when T decreases, reaches its minimum at T_{rev} and then increases below T_{rev} (before reaching the above-mentioned ultra-low- T plateau ϵ''_{plat}). According to the standard TLS model, the ϵ'' decrease above T_{rev} is due to the progressive freezing of the diagonal (or relaxational) part of the response, while the ϵ'' increase below T_{rev} comes from the induced off-diagonal (or resonant) part of the susceptibility: this effect enlarges as T decreases as do all quantum effects. However, due to the quantum nature of ϵ'' below T_{rev} , one expects ϵ'' to be strongly depressed by a strong measuring electric field E at a given T . This can be guessed from the quantum saturation phenomenon which is very general in two level systems [27]. Indeed, increasing E decreases the population difference between the two energy levels: as the Rabi oscillations produced by E on the upper level are in phase opposition with respect to the ones produced on the ground level, the quantum response, once averaged on many independent TLS's, tends to zero when E is increased. Strikingly, Rogge et al. experiments show the opposite trend: $\epsilon''(T < T_{rev})$ increases when E is increased.

As it is carefully explained in Ref. [9], this behavior does not result from heating of the sample by E . To give a supplementary argument with respect to Ref. [9], let us note that if E_{lin} is the upper field below which the dielectric susceptibility is measured as being field independent, one expects that the heating of the sample, for a given $E > E_{lin}$, is more important when T decreases. A heating effect is thus expected to stretch the $\epsilon''(T)$ curve of an

amount increasing as T decreases, i.e. one expects

$$\frac{\partial \chi''}{\partial T} \Big|_{E > E_{lin}} < \frac{\partial \chi''}{\partial T} \Big|_{E = E_{lin}} ; \quad (1)$$

to hold at low T , i.e. mainly at $T = T_{rev}$. As can be seen, e.g. on the Fig. 3 of Ref. [9], the trend of the data is exactly the opposite of Eq. (1). Finally, since heating effects can be ruled out, the fact that below T_{rev} , $\chi''(E > E_{lin})$ does not behave as expected from the quantum saturation phenomenon seems extremely intriguing in the framework of the standard TLS model.

However, this was not pointed out since the non linear effects in the TLS model were, up to now, only calculated by using the adiabatic approximation [11]. Such an approximation states that TLS's are at every moment at thermal equilibrium, i.e., it disregards any coherence effects. It predicts an increase of χ'' with E , i.e. it qualitatively accounts for the experimental behavior. However, in the specific case of the real part of the susceptibility, the consistency of the adiabatic approximation is questionable [12]. Indeed, as it is very clearly stated in Ref. [11], this approximation does not hold for TLS's whose Tunneling energy ϵ_0 is too small, and yet it finds that the nonlinear part of χ'' is dominated by the smallest ϵ_0 values (see after Eq. (3.30) in Ref. [11]). More precisely [11], with $p_0 \neq 1$ D the TLS dipole, even for the lowest electric fields $E \sim 1$ kV/m of frequency $\omega \sim 1$ kHz, the adiabatic approximation fails when $\epsilon_0 < \frac{p_0^2}{\hbar^2 p_0 E} \sim 3$ K, while it is well known, from stationnarity experiments [5], that smaller Tunneling energies exist in glasses. Besides, the second puzzling point is that, according to the authors themselves [11], the reason of the increase of χ'' with E in the adiabatic approximation is physically obscure, which leaves unsolved the question of the expected "quantum saturation effect" above mentioned. Finally, several predictions of Ref. [11] are somehow contradicted by experiments [9]: instead of the predicted T_{rev} / E with $\gamma > 1$, the measured data yield $\gamma < 1=2$; below T_{rev} , at a given E , the predicted peaked behavior of $\chi'' = \chi''(T)$ is not observed; at very low T , the observed E dependence of χ''_{plat} contradicts the predictions.

This work goes beyond the adiabatic approximation, even though, due to the few simplifying assumptions that we have made (see Eq. (2)), we do not intend to yield a fully "from first principle calculation". The key point is that phase coherence is not discarded here since non linear effects are treated by a fully quantum non perturbative method. In the first part, we show that the standard TLS model cannot explain the low-frequency experimental data below 100 mK since it yields, at low T , the above-mentioned quantum saturation phenomenon. In a second part, interactions between defects are added by using an interaction mechanism proposed very recently by Burin et al. [8], and a successful agreement is obtained with experiments. Finally, we briefly discuss experimental predictions implied by Burin et al.'s interaction mechanism.

I. STANDARD TWO-LEVEL SYSTEM MODEL

A. Bloch equations of TLS

1. Dynamics of a unique isolated TLS

Consider a TLS that is sitting in a double-well potential and assume this defect has a dipole moment p_0 . Its energy splitting is related [15] to the asymmetry energy and to the tunneling matrix element ϵ_0 , describing transitions between the wells, by $\epsilon_0 = \frac{p_0^2}{2} + \frac{\epsilon_0^2}{2}$. Due to finite ϵ_0 , the eigen states extend over both sides of the TLS, and the position operator r is no longer diagonal in this eigen basis. As a result, when an external electric field E is applied to p_0 , the coupling Hamiltonian $qE \cdot r$ is not diagonal in the eigen basis [5] (upon which all the operators of this work are expressed), yielding a total Hamiltonian :

$$H = \frac{1}{2} \begin{pmatrix} 0 & 0 \\ 0 & 0 \end{pmatrix} + \frac{p_0 E \cos \omega t}{2} \begin{pmatrix} 0 & 1 \\ 1 & 0 \end{pmatrix};$$

or $H = \frac{\hbar}{2} \mathbf{s} \cdot \mathbf{\omega}$, with $\mathbf{s} = \frac{\hbar}{2} \mathbf{\sigma}$ where $\mathbf{\sigma}$ are the three Pauli matrices and $\mathbf{\omega}$ is an external effective field (components are given below, note $\omega_y = 0$), which shows an effective spin operator \mathbf{s} is associated to the TLS. The systematic use of "spin" language comes from the fact that the three Pauli matrices, combined with the identity matrix, form a general basis for TLS's. Whatever its physical nature, any operator can be expressed as a linear combination of these four matrices, e.g., the density operator can be written : $\rho = (1/2)I + (1/\hbar)S$, where S is the quantum mean value of the spin operator \mathbf{s} . This shows that S_x and S_y describe the coherence effects contained in the off-diagonal

terms of ρ , while S_z is proportional to the population difference between the levels (the occupation probabilities are given by the diagonal terms of ρ).

The movement of ρ_0 and thereafter the dielectric response of the material stem from the dynamics of S . For a perfectly isolated TLS (note that this implies that $T = 0$) the evolution of S in the external field is only a precession around the external field, as can be seen from the Schrodinger equation which leads [5] to $\partial S / \partial t = S \times E$.

2. Dynamics of an ensemble of non-isolated TLS's

At finite T , the dynamics of the TLS must include the relaxation toward its equilibrium value since each TLS interacts with its environment (phonons or neighboring defects). Since these interactions occur randomly for a given TLS, the dynamical equation must deal with ensemble averaged properties S , i.e. with quantities averaged over many similar TLS's. This evolution is given by the Bloch equations, namely

$$\frac{\partial S}{\partial t} = S \times E + \frac{S - \langle S \rangle_{\text{relax}}}{T_{\text{relax}}}; \quad (2)$$

where the last term states that the relaxation of S toward the environment equilibrium values $\langle S \rangle_{\text{relax}}$ must be added to the quantum dynamics (see Appendix A). In Eq. (2) it is assumed that the relaxation of a given S component, say S_x , occurs with a well defined time constant, say T_x . In the important case of short time scales, one needs to go beyond this approximation since echo signals do not generally decay as a simple exponential ([13], [14]). This subtle effect is irrelevant here since, as already stated e.g. in Ref. [5], we are only interested in the long time range solution of Eq. (2), namely $\omega \ll 1/T_{\text{relax}}$ (1 kHz), i.e. we focus on the particular case $\omega \ll 1$ (see below). Similarly the relaxation term of Eq. (2) might become more complicated in the case of very strong fields [36], leading, e.g., to a $S_y = x_{yz}$ term in the relaxation of S_x (see Appendix B). However this should not be the case here since we only focus on the onset of the non linear regime ($\rho_0 E$ will not much exceed $k_B T$). As a result, the relaxation terms can be derived quite simply, as we show now.

i) Phonon induced relaxation.

Let us first focus on phonon field relaxation. The occupation probabilities are altered by the emission or the absorption of phonons, yielding [15] a relaxation of S_z , with the relaxation time $\tau_1 = \tau_1^0 \tanh \frac{\rho_0 E}{2k_B T}$, where τ_1^0 is a sample-dependent constant. Since phonon processes occur randomly and independently for various TLS's, they break the phase coherence of the ensemble of (noninteracting) TLS's, yielding a relaxation time $2\tau_1$ for S_x and S_y . What are the thermodynamic values $\langle S_{xyz} \rangle$ to which S_{xyz} relax? By second order expansion of dynamical correlation functions, it was shown [16] that this relaxation occurs towards the so-called "instantaneous equilibrium values", namely, $\langle S_{xyz}(t) \rangle = \text{Tr}(\rho(t) S_{xyz})$ where $\rho(t) = \exp(-H(t)/k_B T) = \text{Tr}(\exp(-H(t)/k_B T))$ is the "instantaneous" thermodynamical density operator and k_B is Boltzmann's constant. For this result to be valid, several conditions must be fulfilled, among which the most stringent one is, by far: $\rho_0 E \ll \hbar / \tau_c$ where τ_c is the correlation time of the random electrical field acting on a given TLS due to its small interactions with its neighbors (see next paragraph ii)). Finally, these phonon processes yield in the Bloch equations a term $(S_z(t) - \langle S_z(t) \rangle) / \tau_1$ for the population relaxation, and $(S_{xy}(t) - \langle S_{xy}(t) \rangle) / (2\tau_1)$ for the relaxation of the coherence term S .

Does τ_1 depend on time? On one hand, under the above stated assumption $\rho_0 E \ll \hbar / \tau_c$, it was argued [16] that τ_1 does not depend on time (see also Ref. [17]). On the other hand, one may argue [11] that, since the applied electric field modulates the asymmetry energy, one should use $\tau_1(t) = \tau_1^0 \tanh \frac{\rho_0 E(t)}{2k_B T}$, where $E(t) = E_0 + \rho_0 E \cos \omega t$ and $E_{\text{eff}} = \sqrt{\frac{E_0^2}{2} + \frac{\rho_0^2 E^2}{2}}$ arise from the diagonalisation of the total time dependent Hamiltonian H . The use of $\tau_1(t)$ is natural within the frame of the adiabatic approximation [11] where the system is assumed to be at thermal equilibrium at every instant. In our fully quantum approach, the question is much more difficult. In the particular case of the low frequency real part of the susceptibility, however, one can easily explain why using either τ_1 or $\tau_1(t)$ lead to very similar results. Indeed, $\tau_1(t)$ and τ_1 mainly differ only for the TLS's whose gap lie in the range $\rho_0 E$. But, as it will be shown in the insets of Fig. 1 and Fig. 3, the gaps of the TLS's driven in the nonlinear regime by a given E extend on a much larger domain (see sections I.B) and II.B)): this is one of the main results of our fully quantum approach. Thus the possible time dependence of τ_1 is not expected to change the results. This was carefully checked by performing all the calculations reported here twice, once using τ_1 , once using $\tau_1(t)$: the resulting differences between both assumptions turned out in any case to be totally negligible. Hence, throughout the paper τ_1 is considered as time independent, by simplicity.

With the above relations, we get for the diagonal elements $\langle S_{1,1}(t) \rangle$ and $\langle S_{2,2}(t) \rangle$:

$$\langle S_{1;1}(t) \rangle = \frac{1}{2} + \frac{p}{2} \frac{z}{\frac{2}{x} + \frac{2}{z}} \tanh \frac{h}{2k_B T} \frac{p}{\frac{2}{x} + \frac{2}{z}};$$

and

$$\langle S_{2;2}(t) \rangle = \frac{1}{2} - \frac{p}{2} \frac{z}{\frac{2}{x} + \frac{2}{z}} \tanh \frac{h}{2k_B T} \frac{p}{\frac{2}{x} + \frac{2}{z}};$$

For its off-diagonal elements, it is found :

$$\langle S_{1;2}(t) \rangle = \langle S_{2;1}(t) \rangle = -\frac{p}{2} \frac{x}{\frac{2}{x} + \frac{2}{z}} \tanh \frac{h}{2k_B T} \frac{p}{\frac{2}{x} + \frac{2}{z}};$$

where

$$x(t) = \frac{p_0 E}{h} \cos t;$$

$$z(t) = -\frac{p_0 E}{h} \cos t;$$

Finally, one finds for the phonon field contribution:

$$\langle S_x \rangle = \frac{p}{2} \frac{h x}{\frac{2}{x} + \frac{2}{z}} \tanh \frac{h}{2k_B T} \frac{p}{\frac{2}{x} + \frac{2}{z}};$$

$$\langle S_z \rangle = -\frac{p}{2} \frac{h z}{\frac{2}{x} + \frac{2}{z}} \tanh \frac{h}{2k_B T} \frac{p}{\frac{2}{x} + \frac{2}{z}};$$

and $\langle S_y \rangle = 0$.

ii) "Spin-spin" induced relaxation

Let us now turn to "spin-spin" interactions : for a given TLS, the effects of thermal transitions of its neighboring TLS's can be modeled as a small (fluctuating in time) electric field, i.e., as small fluctuating terms $H(t) \ll k_B T$. The latter inequality ensures that the relaxation of the population of the levels (involving S_z) will not be sensitive to $H(t)$. It is shown in the Appendix A that, for a given TLS, the oscillations of $S_{x,y}(t)$ are no longer regular but progressively deformed by the random $H(t)$ terms: due to the absence of correlations between the $H(t)$ values seen by various TLS's, ensemble averaging leads, by cancelation of phases of many TLS's [21], to a relaxation of $S_{x,y}$ to zero (while $S_{x,y}$ remains finite for any given TLS). This happens on a short characteristic time scale $\tau_2 \ll \tau_1^{-1}$ and yields a supplementary $S_{x,y} = 0$ for the relaxation of the coherence terms.

The temperature dependence of τ_2 is not clear at present : in echo experiments [28], [29], both τ_2 / T^{-1} as well as τ_2 / T^{-2} were reported [30]. This might come both from the fact that accounting for the detailed shape of echo signals requires a very subtle theory (see e.g. [13]) and from the fact that several mechanisms contribute to τ_2 . Indeed, the pioneering work [22] of Black et al. predicted a τ_2 / T^{-2} dependence but very recent calculations [23] based upon the mechanism used in part II found that τ_2 / T^{-1} could be justified at low T . Since this new mechanism will be used in the last section, we use throughout this work $\tau_2 = \tau_2 = T$, where τ_2 is a sample dependent constant. In order to try to take into account the various mechanisms which might contribute to τ_2 , the parameter τ_2 will be widely varied, as can be seen in Fig. 2. Last, owing to the smallness of the $p_0 E$ values considered here, we neglect any effect on τ_2 as explained in Appendix B.

iii) Final form of the Bloch equations

Inserting the above relaxation terms in Eq.(2), the three Bloch equations can be written as follows:

$$\frac{dS_x}{dt} - \gamma_z(t) S_y + \frac{S_x - \langle S_x \rangle}{2T_1} + \frac{S_x}{T_2} = 0; \quad (3a)$$

$$\frac{dS_y}{dt} + \gamma_x(t) S_z - \gamma_z(t) S_x + \frac{S_y}{2T_1} + \frac{S_y}{T_2} = 0; \quad (3b)$$

$$\frac{dS_z}{dt} + \gamma_x(t) S_y + \frac{S_z - \langle S_z \rangle}{T_1} = 0; \quad (3c)$$

where all the $S =$ terms come from the relaxation processes, while all the S terms arise from the quantum dynamics, i.e. from the fact that H and S do not commute.

Equations (3a) and (3b) also write

$$\frac{dS_+}{dt} + i\gamma_z(t) S_+ + \frac{S_+}{2T_1} = i\gamma_x(t) S_z + \frac{\langle S_x \rangle}{2T_1}; \quad (4)$$

with

$$S_+ = S_x + iS_y;$$

and $\gamma_{\pm} = \frac{\gamma_1 \gamma_2}{\gamma_1 + \gamma_2}$:

Let us note that γ_{\pm} appears due to the existence in eqs.(3a)–(3b) of the two terms $S_{x,y} = (2T_1)^{-1}$. Even if they are required by consistency (see above and Ref. [24]), these two terms do not exist in the pioneering works accounting either for the small inhomogeneities [5] or for echo experiments [28], [29], [30]. In fact these two terms play a negligible role in the nonlinear susceptibility. To show this, let us first note that as long as $\gamma_1 > \gamma_2$, one gets $\gamma_{\pm} \approx \gamma_2$, i.e. the Eqs. (3a)–(3c) amount to the simpler Bloch equations used before (especially in pulse echo experiments). The key point is that, in the $(\gamma_1; \gamma_2)$ plane, this domain where $\gamma_1 > \gamma_2$ is quite large: it is shown in the inset of Fig. 1 and in Ref. [25] that this domain contains, at least, all the TLS's such that $\gamma_{\pm} = (\gamma_1 T_2)^{-1} = 3$. As shown in the inset of Fig. 1, $\gamma_{\pm} \approx 0.2$ K is much larger than the $p_0 E$ values studied in this work. This indicates that the TLS's standing out of the $\gamma_1 > \gamma_2$ domain should not be affected by E , i.e. they should be in the linear regime (see Ref. [26]). To summarize, nonlinear effects should come mainly from the $\gamma_1 > \gamma_2$ region where the two terms $S_{x,y} = (2T_1)^{-1}$ are negligible. This will be analytically demonstrated in section B) 2).

3. Non perturbative resolution of the Bloch equations

The Bloch equations cannot be solved analytically and even their numerical resolution is so far a great challenge. However, in the audio-frequency range, some approximations can be made which strongly simplify the calculations. As γ_2 is much shorter than the typical time $(\frac{0.1}{\gamma_1})$ to modify the populations, S_z may be considered constant [27] in the right hand-side of Eq. (4). The coherence terms follow adiabatically the population evolution. They reach at every moment the stationary state corresponding to the "frozen" occupation numbers.

Therefore, Eq. (4) can be solved independently of Eq. (3). The stationary solution of Eq. (4) is

$$S_+ = \frac{i\gamma_x S_z + \langle S_x \rangle}{i\gamma_z + 1/T_1}; \quad (5)$$

which inserted into Eq. (3) leads to a differential equation for S_z :

$$\frac{dS_z}{dt} + \frac{\gamma_x^2}{\gamma_x + 1/T_2} S_z + \frac{S_z - \langle S_z \rangle}{T_1} = \frac{\gamma_x \gamma_z}{\gamma_x + 1/T_2} \frac{\langle S_x \rangle}{2T_1}; \quad (6)$$

$S_z(t)$ in Eq. (6) is expanded into its Fourier series to get its stationary state. The expansion is limited to a finite number of harmonics. This number, of the order of 10, is found a posteriori when a stable and accurate result is

obtained. So the differential equation is equivalent to a linear system whose solutions are the harmonics S_z^n . The inverse Fourier-transform gives the periodic evolution of $S_z(t)$. The coherence terms S_x and S_y are deduced from Eq. (5) where $S_z(t)$, the solution of Eq. (6), is inserted. Finally, the first harmonics S_x^1 of $S_x(t)$ is sought, to be included into the dielectric susceptibility (see Eq. (7) below).

Indeed, the susceptibility [5] of a single TLS reads

$$\chi = \frac{2 p_0 j}{E j} \cos \left(\frac{\omega}{h} \right) + \frac{S_z^1}{h} + \frac{S_x^1}{h} ; \quad (7)$$

and it must be averaged over the distribution of TLS's [5] and over the dipole-orientation angle to yield the total susceptibility of the sample :

$$\chi = \frac{1}{P} \int_0^{\omega_{max}} d\omega \int_{\omega_{min}}^{\omega_{max}} d\omega' \frac{d\chi}{d\omega}(\omega; \omega') ; \quad (8)$$

In the remainder of this article, we concentrate on the real part χ' of χ which is linked to the capacitance of the sample, i.e., to its dielectric constant ϵ by :

$$\epsilon = 1 + \frac{\chi'}{\epsilon_0} ;$$

B. The quantum saturation effect: the quantum part of $\chi'(T)$ is depressed by a E increase

1. Numerical results

We have used the standard values for amorphous-SiO₂: $p_0 = 1$ D, $\overline{P} = 3 \cdot 10^{44}$ Jm⁻³, $\omega_1 = 10^8$ sK³ (all the energies in ω_1 taken in K), $\omega_{min} = 10^6$ K, $\omega_{max} = 10$ K, $\omega_{max} = 10$ K. As explained above, we took $\omega_2 = \omega_1 = T$, where ω_2 was ranged from $3 \cdot 10^{11}$ sK to 10^7 sK, allowing to check our fundamental assumption! $\omega_2 = \omega_1$ provided $T = 0.5$ mK. Last, the numerical relative accuracy of our simulations was, in any case, better than 10^{-3} : this was checked very carefully, both by increasing the number of harmonics when solving Eq. (6) and by letting the successive integration procedures converge to better than 10^{-4} . For each set of parameters $E; T; \omega_1; \omega_2; \omega_{min}$ at least $4 \cdot 10^4$ couples of $(\omega; \omega')$ were computed.

The simulations are displayed on Fig. 1. The resonant response (low temperature) is strongly depressed by the drive level, while the relaxation contribution (high temperature) is little affected. This is at odds with the experiments [9] where increasing E leads to an increase of both the resonant response and of its slope $\partial \chi' / \partial T$ below T_{rev} . Let us note that the curve labeled "linear response" was obtained independently by a standard series expansion of the Bloch equations keeping only, as in Ref. [5], the terms proportionnal to E : as E is made very small, the nonlinear calculations very precisely converge towards the linear regime.

However, the extreme sensitiveness of the resonance to the external field is very striking. It decreases rapidly while $p_0 E j < k_B T$. The low-temperature phase-coherent uptum is destroyed by its environment (the external fld), although the perturbation is much smaller than any thermodynamical quantity, which suggests that this effect has a quantum origin. This is further confirmed by the inset of Fig. 2 showing the influence of T and ω_2 on $\chi'(E; T) = \chi'(0; T) = \chi'(0; T)$: for a given E , the smaller T , the larger χ' , which is expected since quantum effects generally increase as T decreases. Similarly, χ' is larger when ω_2 is made smaller, i.e., when quantum coherence is made more "fragile". Finally, the dimensionless χ' appears to depend not only on $E; T; \omega_2$ but also on ω_1 , and it is shown in the main part of Fig. 2 that all these dependencies are a universal function of a dimensionless scale λ , namely, :

$$\chi' = \begin{cases} 0.1 P - & \text{if } \lambda < 1 \\ 0.1 \ln(\lambda) & \text{if } \lambda > 1 \end{cases} \text{ with } \lambda = \frac{p_0 E}{k_B T} \left(\frac{1}{T^2 \omega_2} \right) ; \quad (9)$$

where $\lambda' = 0.45 \pm 0.05$ and $\ln(\lambda)$ might be replaced by a power law of λ with an exponent lower than 0.1. This universal $\chi'(\lambda)$ dependence holds only when the relaxational part of χ' can be totally neglected, i.e., well below $T_{rev} = 50$ mK: in Fig. 2, only data corresponding to $T = 10$ mK have been plotted. For these low T , $\chi'(\lambda)$ remains universal even when $(\omega_1; \omega_2; E)$ are varied over several decades. The factor $\lambda_1 = (T^2 \omega_2)$ in λ becomes very large at low T , yielding nonlinear effects even for very small E : this expresses that the lower T , the smaller the onset field of the nonlinear regime, as already seen on Fig. 1. Let us mention that the data of Fig. 2 correspond to the particular case $\omega_2 = 0$.

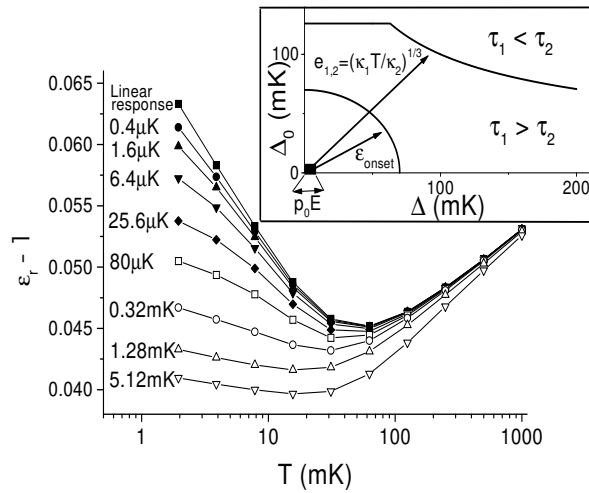


FIG. 1: Inset: At $T = 10$ mK, $\kappa_1 = 10^{-8}$ sK³, and $\kappa_2 = 10^{-8}$ sK, the domain of TLS's such that $\tau_2 < \tau_1$ is quite large and contains all the gaps smaller than $e_{1,2} = (\kappa_1 T / \kappa_2)^{1/3}$ [see [25]]. Even at $p_0 E = 5.12$ mK this domain is larger than the one of the TLS's driven in the nonlinear regime defined by $\epsilon_{\text{onset}} \approx 70$ mK (see Eq. (11c)). Note that $\epsilon_{\text{onset}} \approx p_0 E$ ($p_0 E$ is the small black area very near the origin): this explains that the nonlinear effects are visible even at very low fields, as shown in the main Figure. Main Figure: Dielectric susceptibility of amorphous-SiO₂ at 1 kHz vs temperature simulated at various fields—the value of $p_0 E$ in Kelvin labels each curve—within the standard two-level system model with the following set of parameters: $p_0 = 1$ D, $\kappa_1 = 10^{-8}$ sK³, $\kappa_2 = 10^{-9}$ sK, $\omega_{\text{min}} = 10^6$ K, $\omega_{\text{max}} = 10$ K, $\overline{P} = 3 \cdot 10^4$ Jm⁻³. The low-temperature response vanishes rapidly as the electric field is increased due to the quantum saturation phenomenon. The linear response was obtained by an independent perturbative method.

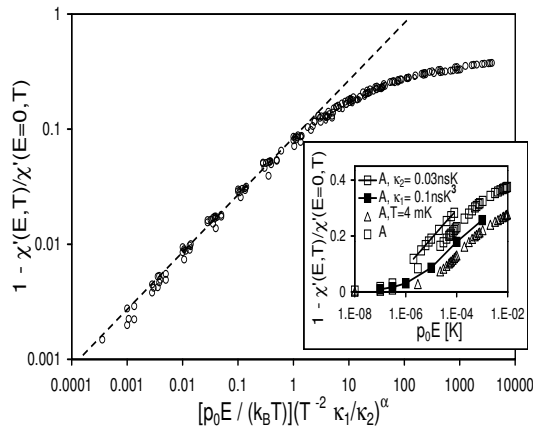


FIG. 2: Inset: $\chi''(E; T) = \chi''(0; T)$ plotted versus $p_0 E$ (in kelvins). Curve A corresponds to $p_0 = 1$ D, $\kappa_1 = 10^{-8}$ sK³, $\kappa_2 = 10^{-9}$ sK, $\omega_{\text{min}} = 10^6$ K, $\omega_{\text{max}} = 10$ K, $\overline{P} = 3 \cdot 10^4$ Jm⁻³ and $T = 2$ mK. The other three curves show the effect upon quantum saturation of the parameter which was changed with respect to A: increasing T , as well as decreasing κ_1 , decreases χ'' ; while decreasing κ_2 increases χ'' , as expected due to the quantum nature of χ'' . Main figure: The various influences of the simulation parameters can be reduced to a universal function of the dimensionless variable $x = \frac{p_0 E}{k_B T} \left(\frac{\kappa_1}{\kappa_2} \right)^{\alpha}$ with $\alpha = 0.45$ numerically. The dashed line shows that $\chi'' / \overline{P} \sim x$ when $x < 1$. The various parameters were ranged over several decades: 10^{10} sK³ κ_1 10^{-8} sK³; $3 \cdot 10^{11}$ sK κ_2 10^{-7} sK; 10^6 K ω_{min} 10^4 K; 10^8 K ω_{max} 3 mK. The data of this figure correspond to the particular case $\alpha = 0$.

2. Physical interpretation

To further understand the universal $\chi''(\omega)$ and demonstrate its quantum origin, let us briefly go into the structure of the Bloch equations. By using the identity $\chi_x < S_z > = \chi_z < S_x >$, Eq. (6) can be written:

$$\frac{dS_z}{dt} + \frac{S_z}{T_1} = \frac{\langle S_z \rangle}{T_1}, \quad \chi_z = \frac{1}{T_1} \left(1 + \frac{1}{2} \frac{(\chi_x T_2)^2}{1 + (\chi_z T_2)^2} \right); \quad (10)$$

In Eq. (10), one gets at $E \rightarrow 0$: $\chi_z = \chi_{z1} = 1/T_1$. As argued in section I A 2), the nonlinear behavior should come from the TLS's such that $\chi_1 > \chi_2$: in this case we see indeed from Eq. (10) that increasing E decreases χ_z much more than χ_{z1} . This strongly depresses the off-diagonal susceptibility, as we show now.

Let us first derive, from Eq. (10), the critical value E_c such that χ_z becomes larger than χ_{z1} : focusing on the gaps lying within the $\chi_1 > \chi_2$ domain, i.e. in the domain where $\chi_2 \ll \chi_1$, E_c is determined by the condition $\chi_1 \chi_2 \ll 1 + \frac{1}{2} \chi_2^2$, yielding:

$$\begin{aligned} \chi_z &= \frac{p_0 E}{k_B T} \quad \text{if } k_B T \gg p_0 E \quad (11a) \\ \chi_z &= \frac{p_0 E}{k_B T} \quad \text{if } k_B T \ll p_0 E \quad (11b) \end{aligned}$$

where all the energies are expressed in kelvins. With the standard values $\chi_1 = 10^{-8} \text{ sK}^{-1}$ and $\chi_2 = 10^{-9} \text{ sK}^{-1}$, we see that $p_0 E$ is much smaller than $k_B T$. Indeed, for $T = 10 \text{ mK}$ we get $p_0 E = 2 \cdot 10^{-5}$ for the smallest gaps following Eq. (11a), and, for example, $p_0 E = 3 \cdot 10^{-3}$ for the gaps $\gg k_B T$ which follow Eq. (11b). Solving Eq. (11b) with respect to E , for a given E , leads to a characteristic gap

$$E_{\text{onset}} = \frac{p_0 E}{k_B T} \quad (11c)$$

where all the energies are in Kelvins. For the highest $p_0 E \approx 5.12 \text{ mK}$ studied here, we get $E_{\text{onset}} \approx 70 \text{ mK}$. As shown in the inset of Fig. 1, E_{onset} is both much larger than $p_0 E$ and corresponds to a domain smaller than the one defined by our assumption $\chi_1 > \chi_2$.

To show that E_c in Eq. (11b) is indeed the critical field for a given TLS, at which the kind of nonlinearities of Figs. 1-2 onsets, let us now compare $\chi''(E) - \chi''(E_c)$ and $\chi''(E)$.

i) If $E = E_c$, we get from Eq. (10) $\chi_z \approx \chi_{z1} \approx 1/T_1$. Solving Eq. (10) is straightforward and leads for the n^{th} harmonics of $S_z(t)$:

$$S_z^n = \frac{\langle S_z^n \rangle}{1 + n^2 \frac{1}{2} \chi_2^2}; \quad (12)$$

where $\langle S_z^n \rangle$ is the n^{th} harmonics of $\langle S_z(t) \rangle$. Remembering that the region of interest is $\chi_z \approx \chi_{\text{onset}}$, it can be checked that $\chi_1 \gg 1$ for basically all the considered TLS's. This yields, from Eq. (12), $S_z(t) \approx \langle S_z^0 \rangle$. Furthermore, since $p_0 E \ll k_B T$ due to Eqs. (11), we get $\langle S_z(t) \rangle \approx \langle S_z^0 \rangle$, which, once combined with the identity $\chi_x \langle S_z(t) \rangle = \chi_z \langle S_x(t) \rangle$, yields $S_z(t) \approx \chi_z \langle S_x(t) \rangle = \chi_x$. Once reported into Eq. (5), this yields:

$$S_x(t) \approx \frac{\langle S_x(t) \rangle}{1 + \frac{1}{2} \chi_2^2} \left(\frac{1}{2} \chi_2^2 \right); \quad (13)$$

where in the last factor the fact that $\frac{1}{2} \chi_2^2 \ll 1$, which holds for any reasonable set of $(\chi_1; \chi_2)$, was used to drop the term χ_2^2 .

ii) For $E = E_c$, we get from Eq. (10), $\chi_{z1} \approx 1/T_1$ and $\chi_1 = 2 \chi_z(t) \approx 2/T_1$. The fact that χ_z is now smaller than χ_{z1} is responsible for the onset of nonlinear effects. This can be seen by setting $\chi_z = 1/2$ throughout the electrical period. With this simplification, one gets, with a derivation similar to the one yielding Eq. (13):

$$S_x(t) \approx \frac{\langle S_x(t) \rangle}{1 + \frac{1}{2} \chi_2^2} \left(\frac{1}{2} \chi_2^2 \right); \quad (14)$$

The off-diagonal part of the response in phase with E is $\chi'' / S_x^1 = E$: it is read directly from Eqs. (13)–(14), remembering that $\langle S_x \rangle = E \cos t$. This yields $\chi''(E = E_0) = \frac{1}{2} \chi''(E = E_0)$, where the factor 1/2 comes from the above relation $\chi_z = \frac{1}{2} \chi_{z1}$, which was a simplification of the case $E = E_0$. The comparison of Eqs. (13)–(14) is thus only semi-quantitative, but it yields the main two features of the quantum saturation phenomenon: first $\chi''(E) < \chi''(E_0)$, second this effect comes from the off-diagonal part of the susceptibility, i.e., it is purely quantum (the diagonal susceptibility $\chi'' / S_z^1 = E$ is much smaller than χ'' / S_x^1 due to the fact that $\omega_1 \ll 1$ below T_{rev}).

We have here an example of quantum decoherence [33]. It is not surprising that these effects were missed by the adiabatic approximation mentioned in the introduction since, in this approach, χ_z has disappeared, yielding for the nonlinear onset [9] no other possibility than $\langle p_0 E \rangle = k_B T$, as expected for a system at equilibrium. Moreover we have shown that the quantum saturation depends on the precise coupling of the three Bloch equations, i.e. of the fact that χ_z evolves faster with E than χ_{z1} : this is out of reach for the adiabatic approximation since it contains only one differential equation [11] instead of Eqs. (3a)–(3c). Finally, the results of Figs 1–2 do not depend on the precise microscopic mechanism involved in χ_z , but only on the fact, well established by echo experiments, that, for a vast subclass of TLS's one has $\chi_z \propto \omega_1$: this is the main reason of the E -induced depression of χ'' of Figs 1–2.

3. Effect of the density of states

More can be learnt from Eqs. (11), and more precisely from Eq. (11b) which holds for the vast majority of the TLS's responsible for the nonlinear behavior. First, let us note that the onset field E_{onset} increases as $\omega_2 = \omega_1$: this suggests that the depression of χ'' , when E is increased, depends on $E \frac{P_{\text{onset}}}{P_{\text{onset}} - 1}$, which, remembering that $\omega_1 = \omega_2$ is the square of a temperature, leads to the dimensionless scale $p_0 E = (k_B T) \frac{P_{\text{onset}}}{P_{\text{onset}} - 1} = (T^2 / \omega_2)$ as the natural parameter for the quantum saturation phenomenon. This dimensionless scale matches exactly the definition of χ'' in Eq. (9).

Second, from the above discussion of Eqs. (13)–(14), the TLS's such that ω_{onset} are already in the saturation regime, while the gaps larger than ω_{onset} are hardly altered by E . It is thus natural to consider the number of TLS's such that ω_{onset} as an estimate of the amplitude of the quantum saturation phenomenon $\chi''(E; T) = \chi''(0; T)$, stating:

$$\chi''(E; T) = \chi''(0; T) / \sum_{\text{min}}^Z \frac{P(\omega)}{P_{\text{onset}} - 1} \quad (15)$$

where the last equality was obtained by using the above-stated relationship E / ω_1 ; while the second equality uses both Eq. (11c) and the fact that the energetic density of states $P(\omega)$ is a constant due to the standard distribution $P(\omega; \omega_0) = P = P_0$. Equation (15) yields exactly Eq. (9) derived from the numerical simulations. This argument enables to state that the small corrections to the standard $P = P_0$ previously proposed only yield small changes to the behavior of Figs. 1–2: this is true, e.g., for the slight depression of the density of states at small gaps derived by Burin [31], as well as for $P = P_0^{1+y}$ with $|y| \ll 1$ proposed in Ref. [32].

To summarize this section I), solving the Bloch equations leads to the quantum saturation effect, i.e., to a strong decrease of the off-diagonal part of χ'' when E is raised. This effect holds for a very large set of ω_1 and ω_2 – the main parameters of the model, and it mainly comes from the TLS's such that $\omega_{\text{onset}} < \omega_{1,2}$. For an ensemble of TLS's with a $P = P_0$ density of states, quantum saturation goes as $E^{0.5}$, and such an exponent justifies a posteriori the nonperturbative character of the method used here. Last, the quantum saturation phenomenon onsets for fields $E = k_B T = p_0$, as seen from Eq. (9). It is thus non-negligible since the field is, in most experiments, decreased well below $k_B T = p_0$. However, in the literature, the trend of the data is systematically the opposite of the one of Figs. 1–2. Since –see Appendix B – more general Bloch equations, corresponding to larger E , should not qualitatively change the results of Figs. 1–2, we conclude that the standard TLS model cannot account for the basic features of the nonlinear experimental data in the kHz range.

II. ADDING INTERACTIONS

A. Burin et al's mechanism

At this step, at least one drive-dependent parameter must be added into the model to explain the large discrepancy with the experimental data. Moreover, it must enhance the relaxation process at low temperature, since coherence is broken by the external field as shown in Figs. 1–2.

Recently, Burin et al. [8] proposed an additional eld-induced relaxation mechanism. They show that the resonant dipole-dipole coupling, which is so small in glasses, can be strongly increased by a low-frequency electric eld. Indeed, thermal excitations, which are at zero-eld localized on each TLS, tend to delocalize by hopping to resonant nearest neighbors. This is due to the fact that resonant hopping demands both TLS's to have very close values of both χ_0 and χ_1 : as the electrical eld modulates the TLS parameter χ , the probability of finding, for a given TLS, a resonant TLS, increases from a negligible value at very low E , to a non-negligible value above a threshold of the external eld. Let us note that this mechanism transports energy; hence it can be treated as a new relaxation mode.

The frequency must be small for the electric eld to have time to modulate the coupling parameters. This is of no consequence here, since our crucial assumption $\omega \ll 1$, leading to Eq. (5), already restricts our work to the low frequency case. Another assumption is that the external eld amplitude is smaller than the characteristic splitting energy $k_B T$, in order to treat the eld as a weak perturbation. The typical values of the frequency and $p_0 E_j$ are respectively 100 Hz and 1 mK but may be softened as a rigorous determination is out of reach.

When the electric eld increases, so does the probability of finding a resonant neighbor close enough to yield tunneling with not too small a probability: the one-particle excitation will relax more rapidly at high E towards another site. One can show the relaxation rate is proportional to the square root of the drive level [8]. To include this new energy relaxation channel, we set in Eqs.(3a)-(3c) $\chi_1^{-1} = \chi_{1ph}^{-1} + \chi_{1B}^{-1}$ where χ_{1ph} is the phonon eld induced relaxation mechanism used throughout section I) and where

$$\chi_{1B}^{-1} = \frac{B}{p_0 E_j^2}; \quad (16)$$

with the constant $B = 10^{-5} \text{ sK}^{1/2}$ for physically reasonable parameters [8]. As a result, increasing E at any given T leads to an increase of the susceptibility χ_0 : this shows that Burin et al.'s mechanism is strong enough to overcome the decrease due to the "quantum saturation phenomenon". However, the agreement between the set of calculated curves (unreported) and the data is very poor since the net increase of $\chi_0(T)$ when E is increased is stronger at high T than at low T . This is due to the fact that, since relaxation dominates the total response, the most important TLS's are such that $\chi_1 \approx k_B T$: their number enlarges with T and so does their supplementary relaxational response due to the new relaxation channel χ_{1B} .

To interpolate between Fig. 1 and Eq. (16) which appear as extreme cases, one might use the very general argument that interaction effects should disappear at high T , e.g., above 100 mK -see Ref. [20]-. This demands that the chosen $\chi_{1B}(T)$ becomes infinite, i.e., negligible, at high T . Such a general requirement can be of course modeled by different laws but all the ones we tried gave the same kind of behavior for the susceptibility. This is why we report on the calculations using a simple law, namely,

$$\chi_{1B}^{-1}(T) = \frac{\chi_{1B}^{-1}}{1 + e^{T_B/T}} \quad \text{with } T_B = 15 \text{ mK}; \quad (17)$$

where χ_{1B} is given by Eq. (16) and the thermally activated behavior models a dipole-dipole coupling constant of $T_B = 15 \text{ mK}$: the energy scale T_B can be deduced from Fig. 3 of Rogge et al.'s data [9] on a-SiO_x since χ_0 becomes T -independent below 15 mK even for E values ten times larger than the range of the linear regime. Of course, this T_B scale can be adjusted empirically since the T where χ_0 becomes T -independent depends on the material. As the coupling constant goes as $g = \frac{1}{r^3}$ and as [5], for a-SiO₂, $g \approx 10 \text{ K nm}^3$, we get a mean distance r_B between interacting dipoles of nearly 10 nm.

B. Numerical results

The modified model predictions using Eq. (17) are displayed on Fig. 3. The values of $p_0 E_j$ have been limited to 10 mK because of the restrictions on both the Bloch equations and the eld-induced mechanism. A trend completely different from the one of Fig. 1 is obtained at low temperature since an increase of the response is observed when the drive level increases.

By computing separately (unreported) in Eq. (8) the two terms of the right hand side of Eq. (7), we checked that χ_x^0 behaves qualitatively as in section I) and that the new trend of Fig. 3 is due to the diagonal part χ_z^0 . To explain this new behavior, one must note that $\chi_{1B}(T)$ is now the upper bound of χ_1 , even for the numerous TLS's whose small χ_0 value lead, in section I), to a very large χ_1 . With $\chi_{1B}(T < T_B) < 1$, the $1 = (\chi_z^2 - \chi_z^1)$ cutoff of S_z seen on Eq. (12) has now disappeared, i.e. the dS_z/dt term in Eq. (6) can be dropped, yielding:

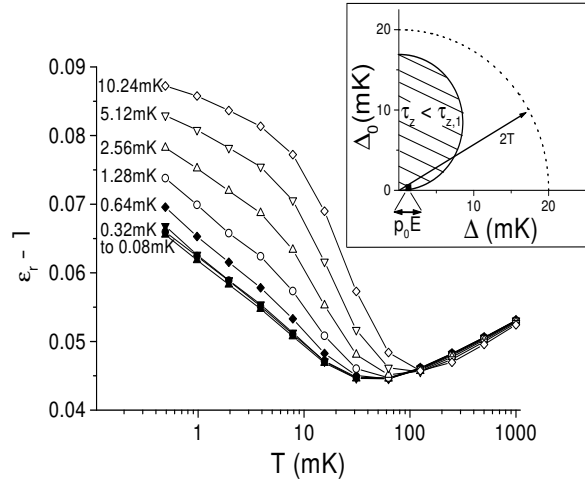


FIG. 3: Main Figure : Simulation of a-SiO₂ susceptibility at 1 kHz vs temperature with Eq. (8) and the same parameters as in the main part of Fig. 1. The calculations were done within a modified TLS model where excitations are no longer localized but can experience field-induced hops to neighboring sites, which is modeled by an additive relaxation channel (see the definition of $\chi_B(T)$ in Eq. (17)). The data show a linear behavior at low enough drive levels (the p_0E values label the curves), an evolution of T_{rev} with E compatible with experiments and a substantial decrease of the T dependence of χ'' at low T ; Inset : For $p_0E \ll k_B T$, in the $(\Delta; \Delta_0)$ plane, $\langle S_z^1 \rangle$ is not negligible only within the $\Delta < 2T$ domain. Even for $p_0E = 0.8$ mK, the hatched area where $z < z_{j1}$ has a non negligible size with respect to this $\Delta < 2T$ domain : this yields a supplementary T -dependent contribution to the diagonal susceptibility χ''_x which overcomes the E -induced depression of χ''_x seen on Fig. 1, and yields the E -enhanced χ'' trend seen on the main part of the figure.

$$S_z(t)' \frac{z}{z_{j1}} S_z(t) ; \quad (18)$$

where $z; z_{j1}$ are defined in Eq. (10). At $E \rightarrow 0$, one has $z' = z_{j1} \rightarrow 1$, yielding with Eq. (18), $S_z(t)' = S_z(t)$. With the additional remark that $S_z^1(\Delta < 2T)' = \hbar p_0 E = (4k_B T)$ while $S_z^1(\Delta > 2T)' = 0$, one gets, with the standard $P = \rho_0$ density of states, that $\chi''_z(T) \propto \ln T$: this is the trend seen above T_{rev} .

To explain the behavior below T_{rev} , the key point is that for quite a large domain in the $(\Delta; \Delta_0)$ one has $z = z_{j1} < 1$: since this factor is T dependent, it will modify the T dependence just above derived for χ''_z from Eq. (18). Focusing on the $\Delta < 2T$ gaps, we get, below T_{rev} , $\chi''_z \propto \chi''_B(T)$ and $\chi''_z \propto T^{-2}$: the condition $z = z_{j1} < 1$ amounts to $\Delta_0 < \frac{2}{x} \Delta^2$, i.e. :

$$2p_0E \propto \frac{P}{\chi''_B(T)} = \frac{2}{x} \sin^2 \theta + \cos^2 \theta \quad \text{with} \quad \theta = \arctan \frac{\Delta_0}{\Delta} ; \quad (19)$$

The $z = z_{j1} < 1$ condition is shown, as a hatched domain, in the inset of Fig. 3. Even for the lowest E studied here, it is not negligible with respect to the $\Delta < 2T$ area. Since in the hatched domain one has $z = z_{j1} \propto \frac{\Delta_0}{\Delta} = \left(\frac{1}{x} \frac{\Delta_0^2}{\Delta^2} \right)$, this factor remains T dependent even below T_B when $\chi''_B(T)$ has reached its maximum value : this is due to the fact that Δ_0 remains T dependent even at very low T . With $S_z^1(\Delta < 2T)' = \hbar p_0 E = (4k_B T)$, integration of Eq. (18) within the hatched area yields a contribution $\chi''_z / E^3 = T^{-1/2}$. Thus: i) this term increases as T decreases; ii) χ''_z increases with E , i.e. it can overcome the E -induced depression of χ''_x . Disregarding the slight difference—see [35]—between the $\chi''_x / E^{1/2}$ seen for the quantum saturation phenomenon and the $\chi''_z / E^{3/4}$, the linear regime of Fig. 3, up to $p_0E = 0.32$ mK can be seen as resulting from the compensation of both effects. At higher E , the χ''_z increase dominates over the E -induced depression of χ''_x , yielding a net increase of χ'' with E . Note that $\chi''_z(E)$ becomes T independent when $T \propto p_0E = k_B$: in this case, indeed, $S_z^1(\Delta < 2T)$ is no longer T dependent. This yields the substantial decrease of the T dependence of χ'' seen for the two highest E values on Fig. 3.

Last, the off-diagonal susceptibility χ''_x / S_x^1 mainly behaves as in section I), i.e. we recover the quantum saturation phenomenon yielding, when E is raised, both a decrease of χ''_x and of the slope $\partial \chi''_x / \partial T$. With respect to section I) the quantum saturation effect is somehow weakened, which can be understood since, for a given E , the number of TLS's lying within the on-set domain of Fig. 1 is larger than the corresponding one in the hatched area of Fig.

3. Finally, the variations of χ'' with T remain smaller than the ones of χ' , excepted in the case where $T < p_0 E = k_B T$: the small T dependence of $\chi''(T < T_B; p_0 E > 5 \text{ mK})$ is thus the only case where χ'' dominates the T behavior of χ' on Fig. 3.

To summarize, the bigger the electric field, the smaller the field-induced relaxation time (see Eqs. (16)–(17)), which enhances the relaxationnal part of the response, leading to a net increase of χ'' with E at a given T . At a given E , when T decreases below T_B , the $\chi''(T)$ increase is due to the fact that χ_2 is still T dependent : this is, of course, out of reach for the adiabatic approximation where χ_2 has disappeared. Finally, inserting Burin et al.'s new relaxation rate in Bloch equations allow to account for the main trend of the nonlinear data : however, in this approach, the so-called "resonant" regime below T_{rev} is not a coherent one but, mainly, a field-enhanced relaxation regime.

C . Comparison with experiments

On Fig. 3, one observes a pseudolinear regime up to $p_0 E \sim 0.05 k_B T$ where the dielectric response is quasi-independent on the external field. This value of the electrical field agrees with the experimental linear regime, which, depending on the materials, extends up to $p_0 E = (k_B T)$ in the range $[0.02; 0.12]$ (see Figs. 3–5 of Ref. [9]). We checked that this pseudolinear regime comes from the form of $\chi_1/B \propto 1/E$ where χ_1 takes the highly nontrivial value $\chi_1 = 2$. Setting lower values for χ_1 , such as $\chi_1 = 0.1$, yields the quantum saturation phenomenon to dominate, leading to the same trends as in Fig. 1, at odds with experiments. Setting $\chi_1 = 1$ leads to the tendency of Fig. 3 but with a linear regime reduced to $p_0 E = (k_B T) < 0.01$. The second key point is the trend of the reversion temperature T_{rev} with E : using Eq. (17), i.e., $\chi_1 = 2$, leads T_{rev} to increase by a factor three when $E = 30 E_{rev}$, where E_{rev} is the electrical field such that the nonlinearities onset at T_{rev} . This is in good agreement with Fig. 3 of Ref. [9]. On the contrary, using $\chi_1 = 1$ leads T_{rev} to increase much faster with E : $T_{rev}(E = 30 E_{rev}) = 30 T_{rev}(E = 0)$. Finally, the key role of $\chi_1 = 2$ is somehow reminiscent of Eq. (9) where $\chi'' \propto 1/E$, even if an analytical argument supporting this idea is still lacking.

With respect to experimental data, a failure, at this step of the discussion, is the ratio between the two slopes $\partial \chi'' / \partial \ln T$ below and above the reversion temperature. In Fig. 3 this ratio is near -1.7:1 instead of -1:1 in most experiments. Furthermore, the low-temperature linear-susceptibility data tend to a T -independent plateau while they do not in our simulations. At very low temperature, interactions are likely to be so strong that the independent TLS model does not apply anymore, even with a renormalized relaxation time such as that of Eq. (17). A transition toward a dipole-glass was invoked to explain the behavior of the samples whose χ'' no longer depends on T below a few mK. In this picture, dipole orientation is progressively frozen, which would lead to a plateau of the susceptibility [6], [39] : by continuity, this would weaken the slope ratio near -1:1. Since the TLS model should not apply at very low T , it is not surprising that the plateau of the susceptibility measured in the nonlinear regime is not well accounted for by Fig. 3. Indeed, Fig. 3 does not show a completely T -independent plateau but only a substantial reduction of the T -dependence of χ'' at low T : as stated in II)B), this is due to χ'' which still exhibits a small T dependence, even when χ'' has turned into its T independent regime. However, if, on Fig. 3, the susceptibility is frozen below a given T , one gets plateaus for χ'' whose heights depend on E , as in experiments. Finally, pushing χ_1 toward 1 strengthens the tendency of χ'' to become T independent at low T (unreported), even if $\chi_1 = 1$ leads to the above-mentioned discrepancies with respect to experimental data. Let us note that some materials (see Rogge et al. [9]) do not yield any sign of such a glass transition even at $T = 0.6 \text{ mK}$.

D . New predictions

Let us move briefly to the physical predictions implied by Burin et al.'s mechanism. Remembering that the inequality $\chi_1 > 1$ allowed the key simplification for the derivation of $\chi''(E; T)$ –see Eq. (5)– we restrict ourselves to the kHz range where this condition is fulfilled. Two main predictions can be done :

i) $\chi_1(B)$ will be suppressed in samples whose thickness h is smaller than the distance B separating the quasi-similar TLS's required by Burin et al.'s mechanism. Indeed, at distances larger than h , dipolar interactions within the dielectric will be suppressed by the screening effect of the numerous electrons of the electrodes. Thus, if $h < B$, one should observe a non linear behavior such as the one calculated in section I) –see Fig. 1–, where the quantum saturation of the levels only remains. In other words, ranging h from a fraction of B to a few B in a series of samples and studying $\chi''(E; T)$ should lead to a gradual transition from Fig. 1 to Fig. 3 if Burin et al.'s mechanism is relevant, while it should not affect the non linear behavior in the standard TLS model. Note that such an experiment looks feasible due to the quite large value of $B \sim 10 \text{ nm}$, –see II)A)–. This is due to the fact that Burin et al.'s mechanism requires the two interacting TLS's to have both very close values of ω and very close values of ω_0 : these conditions are stringent enough to make B much larger than the distance between a given TLS and its nearest neighbor.

ii) The net relaxation frequency $\omega_1^{-1} + \omega_B^{-1}$ of a given TLS increases as E increases. Thus, nonequilibrium data should be of smaller amplitude when E is raised. Indeed, they are currently interpreted as resulting from the very large ω_1 existing in any glass due to the subclass of TLS's whose energy barrier is so high that ω_0 is very small. These very "slow" TLS's have an extremely delayed response to any change of the external constraints, such as the d.c. electrical, or strain, field imposed to the sample: these TLS's yield an excess of states at low energy with respect to the equilibrium density of states, the latter having a small depression at low energies due to TLS-TLS interactions. To our knowledge, the influence of E on nonequilibrium phenomena has been reported only once, in Rogge et al.'s work devoted to nonequilibrium phenomena on a mylar sample [41]. Applying a relative strain field F to the sample leads to a sudden jump of the dielectric capacity C , measured at 5 kHz, followed by a logarithmic relaxation. At $T = 11$ mK, i.e., well below T_{rev} , and with $F = 2.7 \cdot 10^{-6}$, the initial relative jump is $dC/C = 13 \cdot 10^{-7}$ if the measuring field is $E = 5 \cdot 10^4$ V/m (see Fig. 1 of Ref. [41]), while it decreases to $dC/C = 4.5 \cdot 10^{-7}$ if the measuring field is $E = 8.5 \cdot 10^4$ V/m (see Fig. 2 of Ref. [41]). Let us note that, with $p_0 = 1$ D and a relative dielectric constant of 5, $E = 5 \cdot 10^4$ V/m amounts to an energy of 10 mK, of the order of T : in terms of our Fig. 3 this means that one stands just above the pseudolinear regime, i.e., in a regime where our calculations, as well as Burin's mechanism, should apply. Even if this was not investigated systematically, this single experimental datum favors the idea that nonequilibrium effects should be of smaller amplitude when E is increased, due to the interaction-induced reduction of the diagonal relaxation time.

III. CONCLUSIONS

In conclusion, we have simulated the nonlinear dielectric susceptibility of amorphous materials by using the TLS model. Phase coherence effects have been taken into account, which is the main difference with the adiabatic approximation. In the kHz range, the standard TLS model yields a nonlinear behavior at odds with experiments due to the field-induced depression of the quantum response. However, it was possible to fit in many details the experimental low-temperature field-induced rising response by adding a new relaxation mechanism based upon the existence of interactions below 100 mK. In this approach, the low temperature response mainly loses its quantum origin at low frequency. Our work stresses the necessity to inject interactions into the TLS model to get satisfactory predictions.

Acknowledgments

Many thanks to P. Pari, P. Forget, P. Ailloud (CNRS/LPS) and P. Trouslard (CEA/INSTN/IVdG) for help in experiments motivating this theoretical work. Scientific discussions with J. Jorin and J.-Y. Prieur (CNRS, Orsay) turned out to be crucial for this work, as well as the indication of Ref. [27] by P. F. O. H. Rousseau (University of Perpignan). Useful discussions with D. Boutard, M. Ocic, M. Rotter, are also acknowledged.

IV. APPENDIX

A. Phase decoherence induced by small TLS interactions

In this Appendix, we aim at giving some physical insight into the relaxation term introduced in the dynamics of an ensemble of TLS's due to their small mutual interactions. Expanding on the assumption that these interactions are much smaller than the other relevant energy scales (such as T or the gap Δ), the basic idea [16] is to model these interactions by a small random electric field acting on each TLS. This idea is not new [22], [16], and numerical results are presented here only to help understand theoretical results.

1. Interactions effects when the measuring field $E = 0$

Consider first the case where the measuring field $E = 0$. Modeling mutual interactions between TLS's by a random electric field leads, for a given TLS, to a total Hamiltonian given, by :

$$H = \frac{1}{2} \begin{pmatrix} 0 & 0 \\ 0 & 0 \end{pmatrix} + \begin{pmatrix} - & - \\ - & - \end{pmatrix} p_0 E_{rand}; \quad (A1)$$

where the electric field E_{rand} is random in time for the considered TLS, and, at a given instant t , varies randomly for various TLS's. Note that Eq. (A 1) is expressed in the eigen basis of the TLS.

Defining the density operator $\rho(t)$ by :

$$\rho(t) = \begin{pmatrix} \frac{1}{2} + z & x + iy \\ x - iy & \frac{1}{2} - z \end{pmatrix}; \quad (\text{A } 2)$$

it is clear that $x; y; z$ are, respectively, the quantum mean values of the three spin operators ($S_x; S_y; S_z$ are the corresponding symbols once the ensemble average over many similar TLS's is made). By using $\dot{\rho} = [H, \rho]$, where the dot stands for time derivation, the dynamics of $x; y; z$ follows :

$$\dot{z} = -\frac{1}{2} \gamma, \quad \dot{h}_1 = -\frac{1}{2} \gamma E_{\text{rand}} \quad (\text{A } 3a)$$

$$\dot{x} = -\frac{1}{2} \gamma, \quad \dot{h}_0 = +\frac{1}{2} \gamma E_{\text{rand}} \quad (\text{A } 3b) :$$

$$\dot{y} = -\frac{1}{2} \gamma x + \frac{1}{2} \gamma z \quad (\text{A } 3c)$$

To characterize the random fluctuations in time of E_{rand} we model its autocorrelation function by $\langle E_{\text{rand}}(t) E_{\text{rand}}(t + t^0) \rangle_t = \frac{u^2}{p_0^2 c} [\theta(t^0 + c) - \theta(t^0 - c)]$ where $\theta(t)$ stands for the Heaviside step function, c is the characteristic time scale of the fluctuations and $u = \frac{p_0}{c}$ the typical scale of the fluctuating part of the Hamiltonian H . This means that $E_{\text{rand}}(t)$ is drawn at random once every c and can be considered constant over time intervals $[n c; (n + 1) c]$, where n is an integer. Within each of these intervals, $E_{\text{rand}}(t)$ takes the constant value E_n . This allows to solve exactly the equation for y obtained from Eqs. (A 3) : $\ddot{y} + (\frac{\gamma}{2} + \frac{1}{2} \gamma) \dot{y} = 0$. This yields :

$$y(n c + t) = y(n c) \cos \frac{\gamma}{2} t + \frac{y(n c)}{n} \sin \frac{\gamma}{2} t; \quad (\text{A } 4)$$

where $\frac{\gamma}{2} = \frac{1}{2} \frac{u^2}{p_0^2 c}$ with $\frac{1}{2} \gamma$ and $\frac{1}{2} \gamma$ defined as in Eqs. (A 3) by setting $E_{\text{rand}}(n c + t) = E_n$. Inserting Eq. (A 4) into Eq. (A 3a) and Eq. (A 3b), with the notation $X_n = X(n c)$ for any quantity X , we get :

$$\dot{x}_{n+1} = x_n - \frac{1}{2} \gamma \frac{y_n}{n} s_n - \frac{1}{2} \gamma \frac{y_n}{n} (1 - c_n) \quad (\text{A } 5)$$

$$\dot{z}_{n+1} = z_n - \frac{1}{2} \gamma \frac{y_n}{n} s_n - \frac{1}{2} \gamma \frac{y_n}{n} (1 - c_n) \quad (\text{A } 6) ;$$

$$\dot{y}_{n+1} = -\frac{1}{2} \gamma x_{n+1} + \frac{1}{2} \gamma z_{n+1} \quad (\text{A } 7)$$

where $s_n = \sin \frac{\gamma}{2} n c$, $c_n = \cos \frac{\gamma}{2} n c$. The four equations (A 4)–(A 7) allow to deduce $x; y; z$ at step $(n + 1)$ provided the corresponding quantities are known at step n . Choosing the initial conditions $x_1; y_1; z_1$, yields $y_1 = -\frac{1}{2} \gamma x_1 + \frac{1}{2} \gamma z_1$ which allows to initiate the recurrence. Finally, let us note that choosing the initial quantum state as $|j_1\rangle = \frac{1}{\sqrt{2}} (|j_1\rangle + |j_1\rangle)$, where $|j_1\rangle; |j_1\rangle$ are the eigen states of the TLS, amounts to setting : $x_1 = \frac{1}{\sqrt{2}}$, $y_1 = \frac{1}{\sqrt{2}}$, $z_1 = \frac{1}{\sqrt{2}}$.

Figure 4 shows the dynamics of a TLS defined by $\gamma = 1$ K, $c = 0.01$ K evolving from the initial state $a_1 = 1; \gamma_1 = -2$, i.e., from $x_1 = 0; y_1 = -3; z_1 = -4$. The random field characteristics were set to $u = \frac{p_0}{c} = 0.1$ K and $c = h/(4)$, i.e., c was chosen four times lower than the Bohr period. Without 'noise', $y(t)$ exhibits the well-known regular Bohr oscillations (short-dashed line on Fig. 4). The effect of 'noise' is to deform these oscillations (continuous line on Fig. 4) by an amount increasing with time : as a result the periodicity of $y(t)$ gradually disappears. This is illustrated in the inset of Fig. 4 showing the exponential decrease in time of the absolute value $|C_y|$ of the autocorrelation of y , defined by $C_y(t) = \langle y(t^0) y(t^0 + t) \rangle_{t^0} = \frac{1}{2} \langle y(t)^2 \rangle$ with $y(t) = y(t) - \langle y \rangle$ and $\frac{1}{2} = \langle (y^2) \rangle$.

Since the value y_n depends on the set of values E_n drawn for the considered TLS from $n = 1$, ensemble averaging (over many TLS's with the same $\gamma; c$) will lead to a cancellation of y due to the absence of correlations between the noise series seen by different TLS's. This cancellation happens on a time scale τ_2 which should be of the order of the one of C_y shown in the inset of Fig. 4. This cancellation of y after ensemble averaging amounts to a supplementary relaxation term $S_y = \tau_2$ in the Bloch equation describing S_y dynamics.

The dynamics of $x(t)$ (unreported on Fig. 4) is similar to the one of y , yielding a corresponding relaxation term $S_x = \tau_2$. This contrasts totally with the dynamics of $z(t)$, depicted on Fig. 4 : provided the amount of noise $H(t)$ is much smaller than the gap Δ , $z(t)$ stands very close to its initial value z_1 , even at large times. In fact small fluctuations exist, with an autocorrelation decrease similar to the one of C_y , but the key point is that $\dot{z}(t) = \langle \dot{z} \rangle = 0$. Hence the 'noise' does not yield any supplementary relaxation term in the Bloch equation governing the population dynamics S_z .

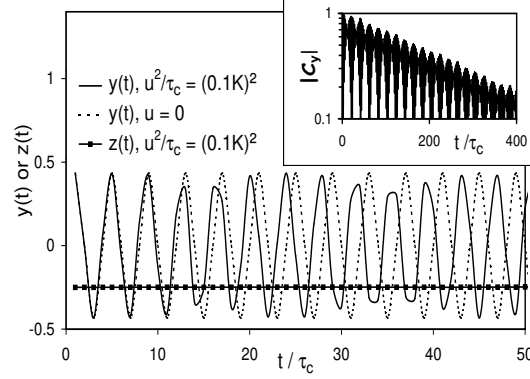


FIG. 4: Dynamics of a TLS ($\omega_0 = 1$ K, $\omega_c = 0.01$ K) submitted to a random electric field ($u^2/\tau_c = 0.1$ K, τ_c is the quarter of the Bohr period $\hbar = \sqrt{\omega_0^2 + \omega_c^2}$). z , the quantum mean value of S_z , is basically constant (solid line with square symbols), i.e., mostly unchanged by the random electric field. On the contrary, y , the mean quantum value of S_y , is strongly affected by random electric field: the periodic Bohr oscillations (short dashed line) seen in the absence of random electric field, are progressively distorted when random electric field is present. Inset: As a result, C_y , the normalized autocorrelation function of $y(t)$, decreases exponentially with time.

2. Interaction effects with a finite measuring field E .

When the measuring E is no longer zero, the whole dynamics should be recalculated, with the supplementary dipolar Hamiltonian corresponding to E . However, the fact that the measuring frequency ω is much lower than ω_0 greatly simplifies the problem. Indeed, if ω were zero, taking into account of E would strictly amount to replace ω_0 by $\omega_0 + \mu_0 E$: with this new definition of ω_0 , all the previous calculations apply, yielding the same relaxation terms in the Bloch equations. We will assume that this holds true for finite ω , due to the fact that for the kHz frequencies considered here, the experimental values of ω_0 ensure $\omega \ll \omega_0$, even at the lowest T studied in the body of the paper.

B. Validity of Bloch equations.

The three Bloch equations Eqs. (3a)–(3c) are valid in the quasilinear response [34]. When the electric field becomes strong enough, the relaxation terms form a nondiagonal matrix, e.g. a $S_z = x, z$ term might come into play in the first Bloch equation, and the corresponding Bloch equations are usually named in the literature Generalised Bloch Equations (GBE). However, up to our knowledge, these generalized relaxation terms have been calculated only in the case of transverse fields in the rotating wave approximation [36]. This is at odds with our physical situation: i) The transverse field case amounts to $\omega = 0$, which, by far, is not the case considered here (remember that, due to the ω_0 density of states, for most TLS's one has $\omega_0 \gg \omega$); ii) The measuring field $E \cos \omega t$ is an oscillating one, not a rotating one $\exp i \omega t$ and the rotating wave approximation would be valid only close to the resonance $\omega' = \omega_0$, a condition totally unrealistic here due to the extreme smallness of $\hbar \omega' = 2 \times 10^{-7}$ K.

However, even if they do not apply in our case, one can use the GBE derived in the rotating wave approximation for transverse fields to guess qualitatively what could be the influence of the off-diagonal relaxation terms. Two points are worth mentioning:

i) One can easily check that the GBE still yield qualitatively the quantum saturation phenomenon, even if the off-diagonal relaxation terms are responsible for quantitative modifications. In particular, it was shown, in the limit of infinite E , that the GBE reduce to the standard Bloch equations with $\omega_2 = 2\omega_1$ and that one gets a vanishing susceptibility.

ii) In the GBE, the off-diagonal relaxation times become infinite (i.e. negligible) when $\omega_c \rightarrow 0$, where ω_c is the correlation time of the random field created, on a given TLS, by its neighbors. In the same spirit [37], in the GBE, ω_2 is affected by a multiplicative factor $1 + \frac{\omega_0^2}{\omega_c^2}$ where $\omega_0 = \mu_0 E / \hbar$ is the Rabi frequency. The order of magnitude of ω_c in glasses was measured only once by Devaud and Prieur [38] who found $\omega_c \approx 10^8$ s at $T = 70$ mK with an expected $\omega_c \propto 1/T$ temperature dependence. The E dependence in the relaxation times can be neglected if $\omega_c \gg 1$.

Aware of these limits, we guess the standard Bloch equations can give a fair approximation as long as $p_0 E_j$ does not exceed 0.1 mK at low temperature. As an additional remark, the validity domain of our calculations extends as ϵ_c decreases.

To summarize, the GBE do not suppress the quantum saturation phenomenon, on the contrary, they are intended to quantitatively account for the various measurable quantities in the saturation regime (such as linewidths, etc...). The problem of the strong depression of χ^0 when $p_0 E_j$ is increased from extremely small values up to $10^{-4} \text{--} 10^{-3} \text{ K}$ is thus unavoidable and is at odds with Rogge et al.'s experiments [9] which were carried out on various glasses and showed absolutely no sign of field induced depression of χ^0 ($T < T_{\text{rev}}$), despite the fact that $p_0 E_j$ was varied from 0.05 mK to 50 mK : the fact that the domain $p_0 E_j \approx 1 \text{ mK}$ was experimentally investigated is of special importance since, as stated above, in this domain, at least, the Bloch equations used here should be valid.

-
- [1] R. Zeller and R. Pohl, Phys. Rev. B 4, 2029 (1971).
 [2] P. W. Anderson, B. I. Halperin, and C. M. Varma, Philos. Mag. 25, 1 (1972).
 [3] W. A. Phillips, J. Low Temp. Phys. 7, 351 (1972).
 [4] J. Joerin and A. Levelut, J. Phys. (Paris) 36, 811 (1976).
 [5] H. Caruzzo, E. R. Gannan, and C. C. Yu, Phys. Rev. B 50, 6685 (1994).
 [6] C. Enss and S. Hunklinger, Phys. Rev. Lett. 79, 2831 (1997).
 [7] E. Thompson, G. Lawes, J. M. Parpia, and R. O. Pohl, Phys. Rev. Lett. 84, 4601 (2000).
 [8] A. L. Burin, Y. Kagan, and I. Y. Polishchuk, Phys. Rev. Lett. 86, 5616 (2001).
 [9] S. Rogge, D. Natelson, B. Tigner, and D. D. Oshero, Phys. Rev. B 55, 11256 (1997).
 [10] G. Frossati, R. Marnard, R. Rammal, and D. Thouleuze, J. Phys. (Paris) 38, L153 (1977).
 [11] J. T. Stockburger, M. G. rifoni, and M. Sassetti, Phys. Rev. B 51, 2835 (1995).
 [12] This contrasts with the dissipative part χ'' of the susceptibility where the adiabatic approximation seems more efficient, which is not surprising since it is well established that both parts of χ are not dominated by the same kind of TLS's.
 [13] B. D. Laikhtman, Phys. Rev. B 31, 490 (1985).
 [14] Yu. M. Galperin, V. L. Gurevich, and D. A. Parshin, Phys. Rev. B 37, 10339 (1988).
 [15] W. A. Phillips, Rep. Prog. Phys. 50, 1657 (1987).
 [16] A. Abragam, The Principles of Nuclear Magnetism (Oxford University Press, London, 1961).
 [17] The other underlying key assumption is that the phonon density remains at equilibrium when a phonon is emitted or absorbed. This assumption may fail if the time for the emitted phonon to be thermalized is not negligible, inducing a local nonequilibrium phonon density called "bottleneck effect" [18]. However, this effect has not been observed in glasses [19], suggesting τ_1 is indeed time-independent.
 [18] P. L. Scott and C. D. Jeries, Phys. Rev. 127, 32 (1962).
 [19] C. C. Yu and A. J. Leggett, Comments Cond. Mat. Phys. 14, 231 (1988).
 [20] P. Neu, D. R. Reichman, and R. J. Silbey, Phys. Rev. B 56, 5250 (1997).
 [21] Y.-K. Yu, Phys. Rev. Lett. 85, 4199 (2000).
 [22] J. L. Black and B. I. Halperin, Phys. Rev. B 16, 2879 (1977).
 [23] A. L. Burin, Y. Kagan, L. A. Maksimov, and I. Y. Polishchuk, Phys. Rev. Lett. 80, 2945 (1998).
 [24] In the case of strictly non interacting TLS's, χ_{xy} becomes infinite and the relaxation of both S_x and S_y is only ensured by the $S_{xy}=2\tau_1$ terms.
 [25] With $\tau_2 = \tau_1$ and $\tau_1 = \tau_1^0 \tanh \frac{\epsilon_2}{2k_B T}$, the domain $\tau_1 > \tau_2$ is found as follows: i) if $\epsilon_2 < 2k_B T$, this amounts to $\tau_1^0 = (2\tau_2)^{-1} \approx 2 \text{ K}$, a condition basically always fulfilled since ϵ_{max} is hardly above this energy scale; ii) if $\epsilon_2 > 2k_B T$, one gets $\tau_1^0 < \tau_1 T = \tau_2$ which amounts either to $\tau_1^0 = (\tau_1 T = \tau_2)^{-1=3}$ in the case where $\epsilon_2 < \epsilon_{1,2}$, or to $\tau_1^0 = \tau_1 T = (2\tau_2)$ in the case where $\epsilon_2 > \epsilon_{1,2}$. Combining these conditions yields the upper curve of the inset of Fig. 1 and one sees that the domain $\tau_1 > \tau_2$ contains, at least, all the gaps $\epsilon_{1,2}$.
 [26] Since the TLS's out of the $\tau_1 > \tau_2$ domain are in the linear regime, one can use Ref. [5] to compute their susceptibility χ_{lin}^0 . In Ref. [5], it appears that χ_{lin}^0 does not depend on τ_2 for the TLS's such that $\tau_2 \gg \tau_1$, a condition easily obeyed when $\epsilon_{1,2}$: for these TLS's the difference between τ_1 and τ_2 does not matter. Thus, Eqs. (3a)–(3c) amount to their simpler form used before [5]. Remembering that it was shown to be true also for the TLS's lying within the $\tau_1 > \tau_2$ domain, we conclude that our Eqs. (3a)–(3c) and their simpler form used before lead to the same results for χ^0 calculations and not only for the nonlinear part of χ^0 . This holds provided that the parameters τ_1, τ_2 are taken in physically reasonable intervals, such as the ones used in Figs. 1–2.
 [27] C. Cohen-Tannoudji, J. Dupont-Roc, and G. Grynberg, Atom-Photon Interactions (John Wiley and Sons, New York, 1992).
 [28] L. Piche, J. Phys. (Paris) 39, (C6)1545 (1978).
 [29] L. Bernard, L. Piche, G. Schumacher, and J. Joerin, J. Low Temp. Phys. 45, 411 (1979).
 [30] J. E. Graebner and B. G. Golding, Phys. Rev. B 19, 964 (1979).
 [31] A. L. Burin, J. Low Temp. Phys. 100, 309 (1995).
 [32] G. Frossati, J. Le G. Gilchrist, and W. Meyer, J. Phys. C: Solid State Phys. 10, L515 (1977).

- [33] A. J. Leggett, S. Chakravarty, A. T. Dorsey, M. P. A. Fisher, A. Garg, and W. Zwerger, *Rev. Mod. Phys.* 59, 1 (1987).
- [34] R. G. DeVoe and R. G. Brewer, *Phys. Rev. Lett.* 50, 1269 (1983).
- [35] The $E^{3=4}$ exponent is not exact since, in the Fourier Transform of Eq. (18), we neglected the fact that $\omega_z = \omega_{z,1}$ is time dependent and that all its harmonics couple to $\langle S_z^n \rangle$ to contribute to S_z^1 .
- [36] E. Geva and R. Koslo, *J. Chem. Phys.* 102, 8541 (1995).
- [37] K. Wodkiewicz and J. H. Eberly, *Phys. Rev. A* 32, 992 (1985).
- [38] M. Devaud and J.-Y. Prieur, *Europhys. Lett.* 6, 523 (1988).
- [39] A. Wurger, *From coherent tunneling to relaxation, dissipative quantum dynamics of interacting defects* (Springer, Berlin, 1997).
- [40] M. von Schickfus and S. Hunklinger, *Phys. Lett.* 64A, 144 (1977).
- [41] S. Rogge, D. Natelson, and D. D. Osheroff, *J. Low Temp. Phys.* 106, 717 (1997).